Dutra, J. R., Moni Ribeiro Filho, S. L., Christoforo, A. L., Panzera, T. H., & Scarpa, F. (2019). Investigations on sustainable honeycomb sandwich panels containing eucalyptus sawdust, Piassava and cement particles. *Thin-Walled Structures*, *143*, [106191]. https://doi.org/10.1016/j.tws.2019.106191

University of Bristol - Explore Bristol Research
General rights

Investigations on sustainable honeycomb sandwich panels containing *Eucalyptus* sawdust, *Piassava* and cement particles

Jezrael Rossetti Dutra[1], Sergio Luiz Moni Ribeiro Filho[1], André Luis Christoforo[2],

Tulio Hallak Panzera[1*], Fabrizio Scarpa[3]

[1] Centre for Innovation and Technology in Composite Materials (CITᵉC), Department of Mechanical Engineering, Federal University of São João del Rei (UFSJ), Brazil.

Corresponding author*: panzera@ufsj.edu.br

[2] Department of Civil Engineering, Federal University of São Carlos, Brazil.

[3] Bristol Composites Institute (ACCIS), University of Bristol, UK.

Abstract: A full factorial design is performed to investigate a sandwich structure consisted of *Piassava* fibre laminates as face sheets and epoxy-based honeycomb cores containing *eucalyptus* sawdust and cement particles. A three-point bending test is used to evaluate the composite structure. The composite setup which achieves higher flexural modulus and strength is used as honeycomb core material. Finite element models are developed to predict the failure and the elastic flexural properties of the sandwich panels. The validated FE model is used to perform a parametric analysis identifying the effect of geometric variations on the flexural performance. The results reveal that the constructive parameters significantly affect the core shear stress, facing stress, flexural stiffness and strength in different ways and intensities.

Key-words: Piassava fibres; *Eucalyptus* sawdust; honeycomb sandwich panels; finite element analysis; design of experiment (DoE); parametric analysis.

1. INTRODUCTION

The honeycomb sandwich structures have been extensively investigated and analysed for great diversity of topologies [1-2] and material composition [3-5]. Innovative sandwich panels based on hybrid composites have gained new achievements for a range of different engineering applications, mainly due their lightweight and unpredictability of mechanical behaviours. The behaviour of sandwich panels has been optimized for different loads and applications, reaching new boundary conditions for promising multifunctional applications, such as airplane, marine and train structures [6]. In particular, the combination of composite facings reinforced with natural fibres and

honeycomb core has the potential to develop alternatives for low cost components in secondary structural technologies and lightweight transportations. Sun *et al.* [7] investigated the crashworthiness characteristics and collapse mechanism via three-point bending and in-plane compression in aluminium honeycomb sandwich panels. Wang, Li and Xiong [8] evaluated the bending performance of a ceramic honeycomb sandwich panel. The authors performed parametric analyses and finite element models to further explore the effects achieved by the ceramic face-sheet and the honeycomb core.

Hybrid composites made with wood sawdust, cement particles and natural fibres can be considered an innovative design for new eco-friendly construction applications, which minimize the consumption of synthetic raw materials and preserve natural resources [9]. Wood sawdust is one of the lignocellulosic biomasses obtained from the processing of wood in various useable sizes [10-11]. The production of wood waste is up to 24.15 million m^3 per year, in which a large amount is burnt or landfilled [10]. In the wood-furniture production chain it is estimated that only between 30% to 60% of a tree is tapped. In general, the wood residue is in the form of sawdust and chips which are discarded in the trash or burned for energy production. In recent years, sawdust disposal has received more attention in response to growing environmental concerns and advances in science. The sawdust consists of lignin, cellulose and hemicellulose, which in principle can be used to produce fuel [12], fertilizer [13], filler of polymers [14-15] and composites [16-17] and others. Dai and Fan [10] have investigated biocomposites based on wood sawdust with novel modification and gypsum. Perez *et al.* [16] have evaluated the effect of maleic anhydride grafted PP (MAPP) on the polypropylene/wood flour composites. The presence of MAPP has increased the tensile strength (34.67 MPa) and ductility of the composites. Ku *et al.* [17] found that the stiffness of microwave-cured sawdust reinforced vinyl ester composites is higher than those cured at room temperature. Missagia *et al.* [18] revealed that the epoxy composite containing 30 wt% of *Eucalyptus grandis* sawdust with a particle size range of 50-80 US-Tyler increased its compressive stiffness.

The use of cement particles in the polymer matrix has proven to be a feasible solution to enhance the mechanical and physical performance of hybrid composites. The effects of Portland cement inclusions into hybrid composites have been reported by Melo *et al.* [19], Torres *et al.* [20] and Ribeiro Filho *et al.* [21], leading to an increase in mechanical properties. Melo *et al.* [19] reported that the cement particles increased flexural strength and flexural modulus of glass fibre reinforced composites. Higher

mechanical properties were observed at 28 days of cure time, especially in those composites produced with 2.5 wt% of cement particles. Torres *et al.* [20] also found that cement inclusions increase the flexural stiffness and strength of unidirectional glass fibre laminates. A substantial increase in impact resistance and flexural properties was achieved when 5wt% of cement particle was added. Ribeiro Filho *et al.* [21] revealed that the presence of cement particles increases the stiffness and flexural strength, apparent density, apparent porosity and water absorption of hybrid composites containing unidirectional sisal and glass fibres.

Piassava (*Attlalea funifera Mart*) is a Brazilian abundant palm species, which has long, hard and tough fibres that provide moderate mechanical properties [22]. It is estimated that 20% of Piassava fibres are eliminated during the production chain of brooms, brushes and kiosks coverage [23]. The replacement of synthetic fibres by natural fibres has been extensively investigated in the composite field. Natural fibres are widely attractive as reinforcement in composite materials because of their low cost, moderate strength and sustainable features. Piassava fibre has been used as a reinforcing phase in a variety of polymer composites [9, 11, 24]. Elzubair *et al.* [25] reported the morphological, mechanical and thermal characterization of two species of *Piassava* fibres. Elzubair and Suarez [22] evaluated the mechanical properties of composites consisted of high-density recycled polyethylene (HDPE-r) reinforced with untreated and treated (silane and NaOH) Piassava fibres. The increase in fibre content led to a gradual change in fracture mechanisms and mechanical properties.

The present work investigates a novel honeycomb sandwich panel made with Piassava fibre composite facings and non-metallic core consisted of *eucalyptus* sawdust, Portland cement and epoxy polymer. This new concept of honeycomb sandwich can be considered a feasible eco-friendly alternative to develop lightweight transportations, such as bus, train and automobile. Rectangular and hexagon honeycomb cells are assessed via three-point bending test. Sandwich panels are produced by bonding two layers of Piassava laminates to the honeycomb cores. Bending tests are carried out to validate the Finite Element model and subsequently, a parametric analysis is conducted to determine the effect of the honeycomb thickness – T direction (5, 10, 20 and 30 mm), core cell configurations (hexagon and rectangular), cells per honeycomb (42, 84 e 126 cells), core cell thickness (1, 2, and 3 mm) and Piassava laminate facing thickness (1 and 2mm) on the mechanical responses of the sandwich beams.

2. MATERIALS AND METHODS

2.1 Facing material: Piassava laminate composites

A biocomposite made with unidirectional Piassava fibres and Araldite-M (RenLam[©] M-1, Huntsman) epoxy polymer is used as honeycomb facings. Preliminary tests are conducted to set the amount of Piassava fibres specially to avoid micro voids in the composite surface. A fibre/polymer volume ratio of 40/60 is considered in the experiment. The Piassava fibres are supplied by a local producer in Minas Gerais (Brazil). Pre-stressed unidirectional Piassava fabrics are manually produced using a stretcher made of wood and fastening components as shown in Figure 1a. The epoxy polymer is mixed manually using a resin/hardener ratio of 5:1 for 5 min at 20°C and 55% RH. A hand lay-up technique is used to fabricate two-layer composites with pre-stressed Piassava fibres (Figure 1b).
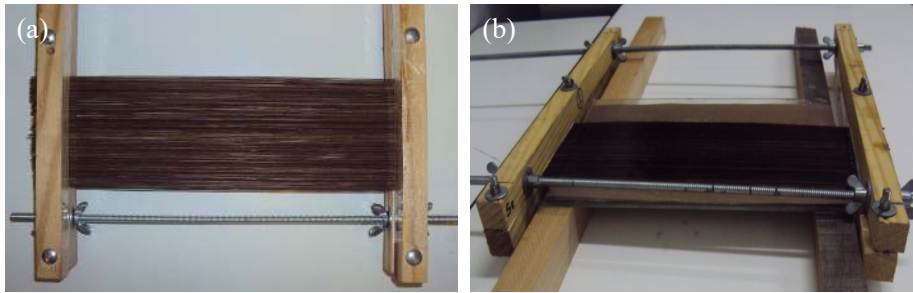

Figure 1. Piassava weaving (a) and composite lamination (b).

2.2 Honeycomb core material: hybrid composite

A three-phase composite is used to fabricate the honeycomb cores. The sawdust obtained from *Eucalyptus* wood is supplied by Agostini Company (Brazil). The wood powder is washed, and oven dried at 60°C for 12 hours. Portland cement (ASTM III) is supplied by Holcim (Brazil). The wood particles are classified by sieving process in a size range of 50-80 US Tyler (0.297-0.177 mm).

Portland cement is combined with sawdust particles at two levels: 5 wt% and 10 wt%. The Araldite-RenLam[©] M-1 (Huntsman) epoxy polymer is prepared by mixing resin and hardener at a ratio of 5:1 for 5 min at 22°C and 59% RH. Subsequently, the particles and the epoxy polymer are hand-mixed for 5 min. The mixture is poured into a rectangular mould (Figure 2a) to produce prismatic samples (50.8 × 12.7 × 1.6 mm^3) for the flexural test (ASTM D790 [26]), as shown in Figure 2b. A Shimadzu test machine

(AG-X Plus) with 100kN load cell is used. A test speed of 2 mm/min with a nominal length of 25.4 mm is considered.
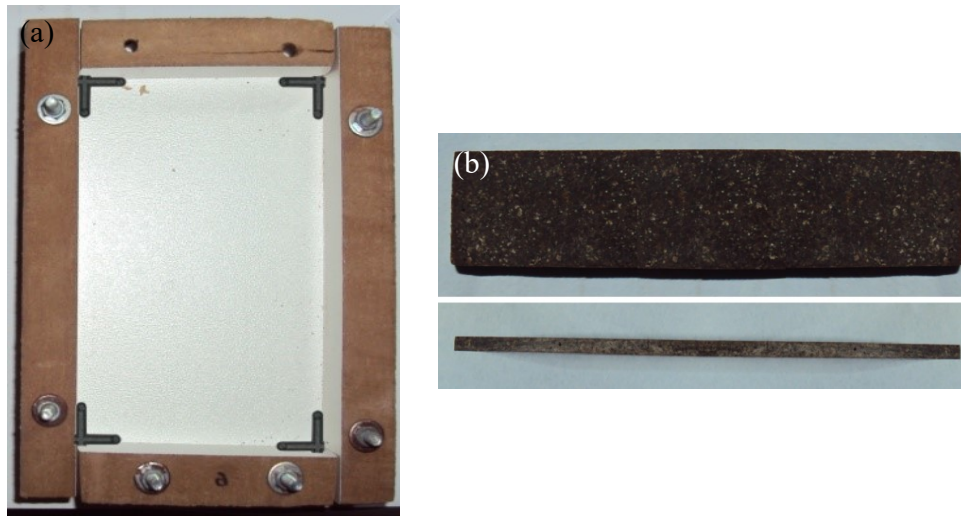

Figure 2. Wooden mould (a) and particulate composite (b).

The factorial design (n^k) is essentially composed of all possible combinations of the factors (k) and its respective levels (n), which allow to identify the most significant factors and their interactions in the process. A full factorial design of $2^1 3^1$ is performed to investigate the effect of wood sawdust/epoxy resin (40/60 and 20/80 wt%) and Portland cement inclusions (0, 5 and 10 wt%) on the flexural properties of hybrid composites. The amount of cement (5 or 10 wt%) is calculated based on the amount of polymer (60 or 80 wt%). Table 1 shows the experimental planning matrix. Five samples are fabricated for each experimental condition and replicated (2 replicates). The best setup condition in terms of higher mechanical properties is used to fabricate the honeycomb cores.

Table 1. Full factorial design for particulate composite.

Experimental condition	$\dfrac{\text{wood sawdust}}{\text{epoxy resin}}$ (wt%)	Cement inclusion (wt%)
C1	40/60	0
C2	40/60	5
C3	40/60	10
C4	20/80	0
C5	20/80	5
C6	20/80	10

2.3 Sandwich panels

Sandwich panel facings are made from two-layer Piassava laminates, while honeycomb cores are made from hybrid composites previously investigated (Figure 3a).

Honeycomb cores are fabricated with rectangular and hexagonal cell configurations. The honeycomb cells (Figure 3c) are manufactured using silicone moulds obtained via polypropylene-PP models (Figure 3b) machined using 3D CAD/CAM technique. Six samples for each configuration are fabricated to perform the flexural tests according to the ASTM C393 standard [27]. An Instron test machine (model DL 500) with a load cell of 5 kN at 2 mm/min is used to carried out three-point bending tests (see Figure 4).
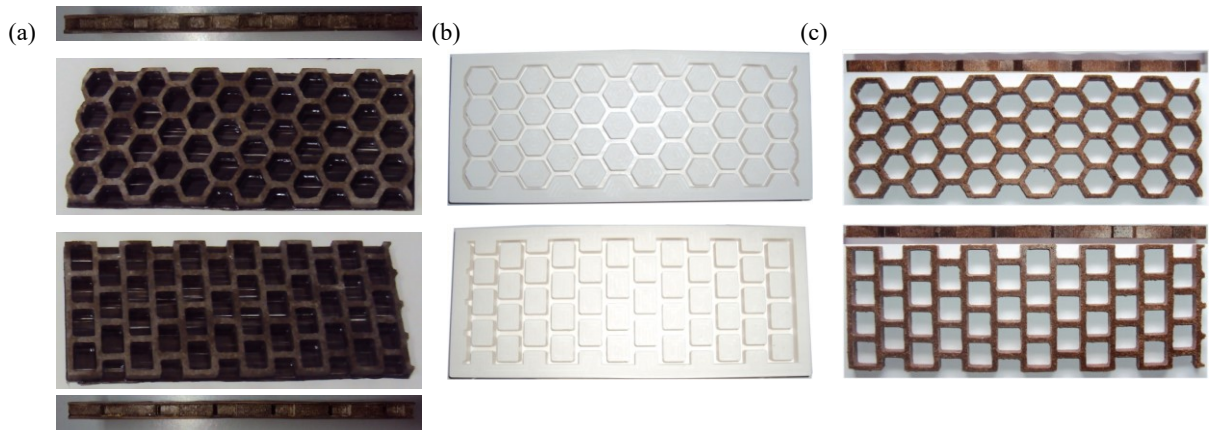

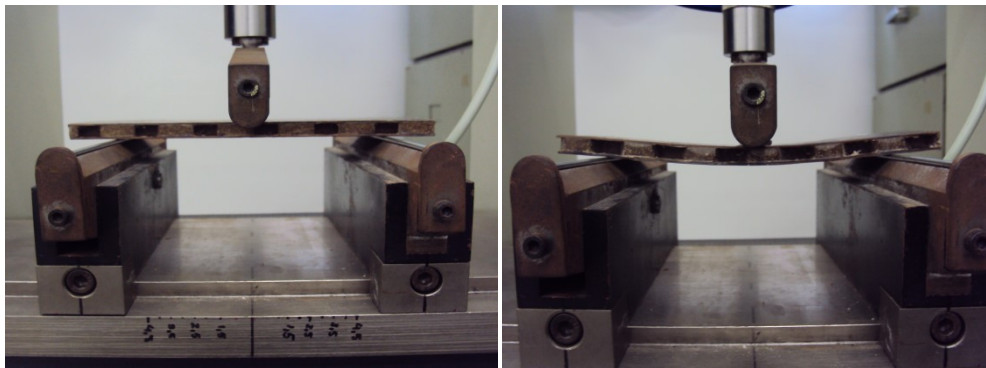Figure 3. Sandwich panels (a), polypropylene-PP models (b) and honeycomb cells made with hybrid composites (c).

Figure 4. Experimental tests of sandwich panel.

2.4 Finite element method

The Finite element analysis (FEA) is performed to predict the maximum deflection of the sandwich panel under three-point bending test. The finite element representative 3D-honeycomb model is composed of two layers of Piassava laminate with a hybrid composite honeycomb core (Figure 5). The eight-node type C3D8R with hourglass control is adopted to mesh all computations. The mesh conversion study is adopted to obtain a balance between numerical robustness and computational efficiency in convergent solution.
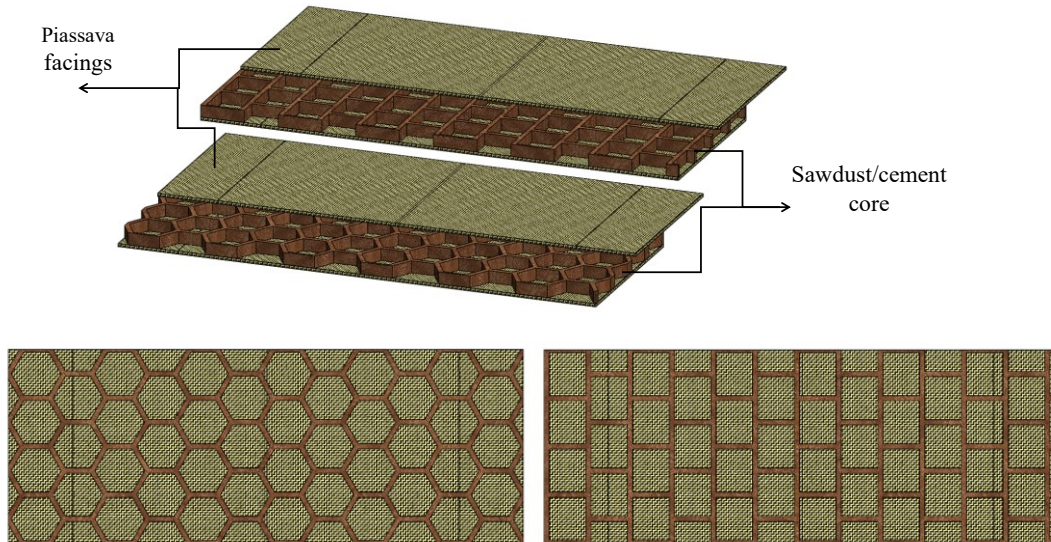
Figure 5. Schematic piassava reinforced sawdust/cement honeycomb sandwich.

The Abaqus/Standard model is solved by the static-general procedure employing the quasi-static approach. The sandwich structure is loaded centrally by a rigid cylindrical indenter through an area of 1×75 mm^2 with 2 mm/min, while the supports are constrained in the xz plane, restricting translation only in the y direction (Figure). The geometry profile for FEM is based on the recommendations of ASTM C393 [27]. The interface region between the facings and the core was modelled using the cohesive elements, which is able to describe the relationship between the interfacial force and the displacement of the crack opening (delamination). The plies with cohesive elements are modelled to evaluate delamination failure (Figure 7). A C3D8R hexahedral elements is used in the facings and in the core because of the better compatibility with the cohesive elements. The parameters of the cohesive zone model in the response of piassava-epoxy are approximated by the model presented by Dadej and Surowska [28]. The values of penalty stiffness, damage initiation stress and fracture energy are $K_{nn} = K_{ss} = K_{tt} = 10^5$ N/mm^3, $t_{nn} = t_{ss} = t_{tt} = 100$ N/mm^2 and $G_{1c} = G_{11c} = G_{111c} = 3.8$ N/mm, respectively. The Maximum Stress Criterion (MAXS) method available in Abaqus is used as the associated beginning of the cohesive element degradation. The contact surface to surface is defined between the indenter and the top layer with a coefficient of friction of 0.10.
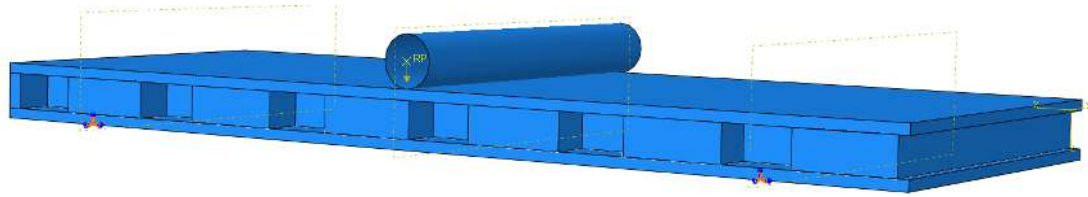
Figure 6. Boundary conditions of uniaxial bending simulations.
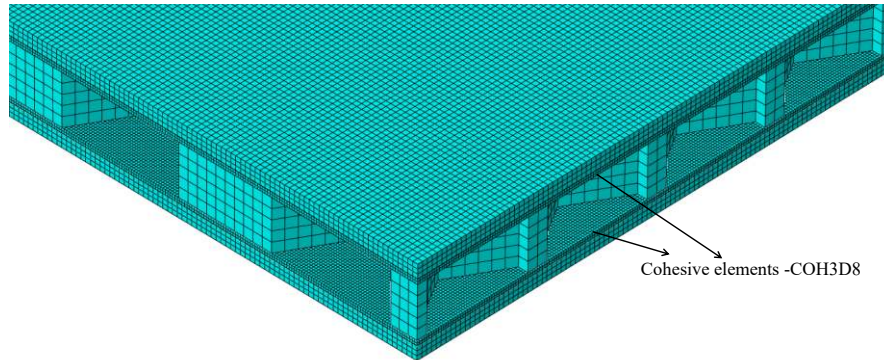

Cohesive elements -COH3D8

Figure 7. Details of the cohesive elements in the Finite Element Model.

The mechanical properties of the piassava skins and sawdust-cement core are calculated according to the three-point bending test and the micromechanical analysis of the composites considering the anisotropy (Table 2). The modulus of elasticity and the Poisson´s ratio are obtained via tensile tests performed on a Shimadzu testing machine (AG-X) equipped with a 2D video system (Figure 8). The fracture strength required for the description of the finite element analysis is obtained in the literature [11, 29]. This value is slightly approximate and calibrated considering the presence of cell defects caused by the manufacturing process. These values are incorporated into the FE models being validated using the experimental data acquired through bending tests. The hybrid sawdust-cement core can be considered a brittle material, so the failure mode applied in numerical analysis is Brittle Cracking. In this approach, the material fails if the maximum stress of the integral point on the element exceeds the fracture strength.

Table 2. Mechanical properties of the composites.

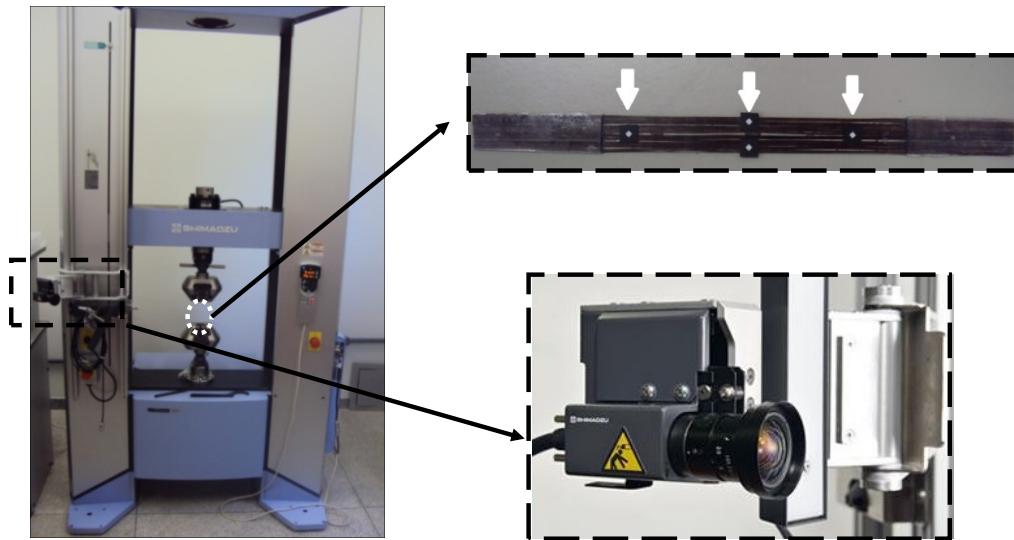| Properties	Piassava Laminate	Hybrid composite	Unit
E_1	3445	2890	MPa
E_2	354.45	315	MPa
E_3	354.45	315	MPa
Nuf_{12}	0.33	0.36	
Nuf_{13}	0.33	0.36	
Nuf_{23}	0.66	0.72	
Density	1.17	1.43	g/cm³
Fracture Strength	152.7	61.3	MPa

Figure 8. Experimental setup for the tensile tests.

2.5 Parametric analysis

Figure 9 shows the experimental and numerical curves achieved for rectangular and hexagonal honeycomb panels. The experimental deflection and the deformation process show good accurate match as shown in Figure 9. Based on the validated FE model, a parametric analysis is performed to predict the optimal configuration of the sandwich panel to maximize mechanical performance. The finite element models are parameterized based on cell height - T direction (5, 10, 20 and 30 mm), honeycomb geometry (hexagon and rectangular), cells per honeycomb (42, 84 and 126 cells), web thickness (1, 2 and 3 mm) and facing thickness (1 and 2 mm), as shown in Table 3. The dimensions of the panels are based on the recommendations found in ASTM C393/C393M [27]. Figure 10 illustrates the geometric configurations of the sandwich panel used in parametric analysis.
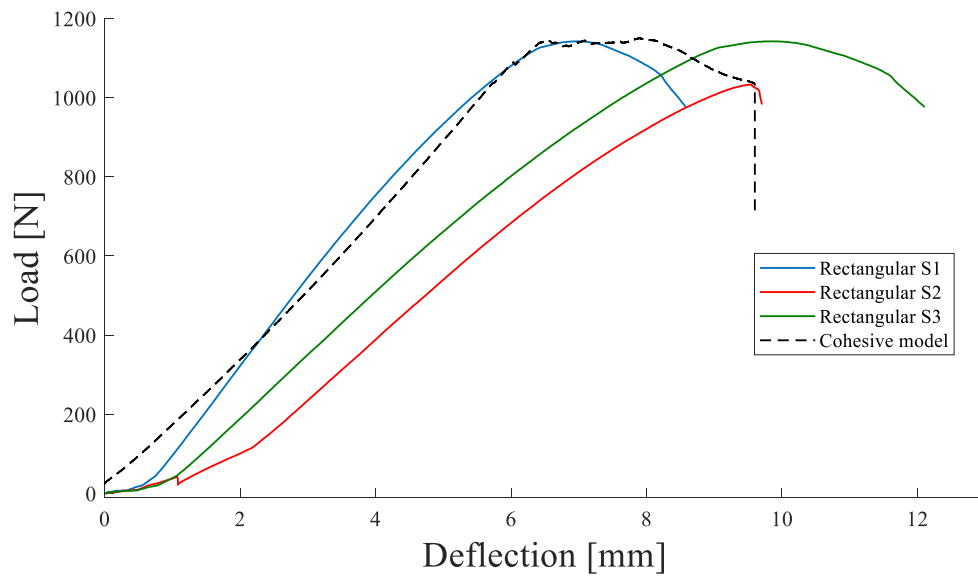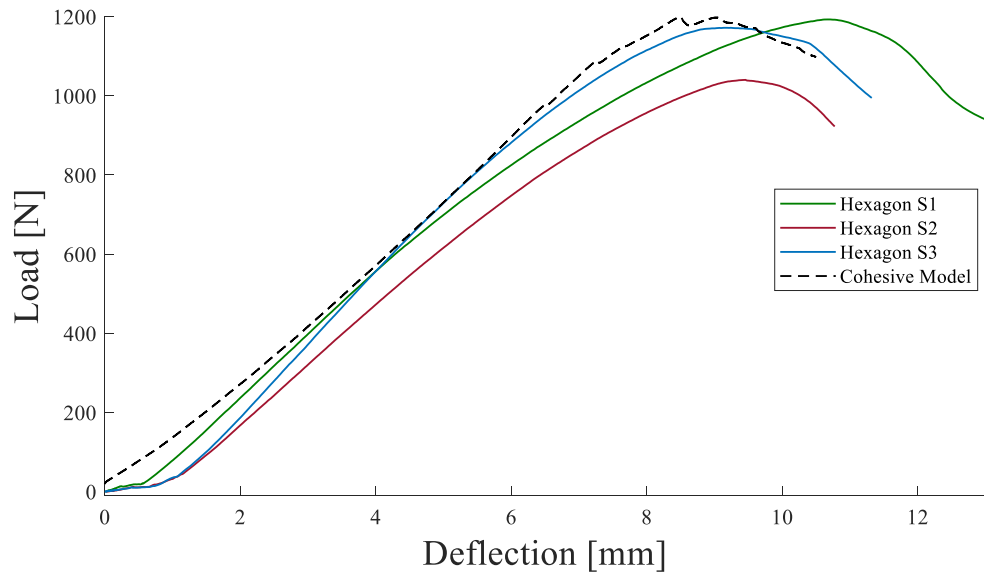
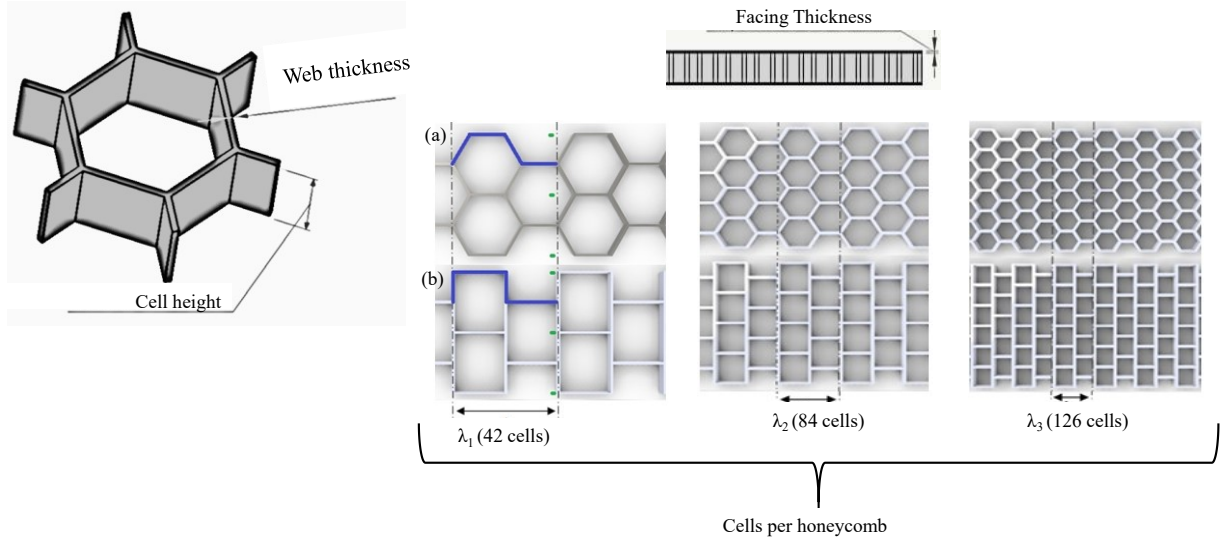Figure 9. Correlation between experimental results and FEA approach.

Figure 10. Geometric factors of the honeycomb core composite sandwich.

Table 3. Parametric conditions for the FE model representing the honeycomb sandwich.

Geometric factors	Levels			
Cell height [mm]	5	10	20	30
Honeycomb geometry	Hexagon		Rectangular	
Cells per honeycomb	42	84		126
Web thickness [mm]	1	2		3
Facing thickness [mm]	1		2	

The mechanical parameters corresponding to the responses of the parametric analysis are the core shear ultimate and facing stresses (F_s^{ult} and σ, respectively, determined by the ASTM C393 [27]), and the flexural stress (σ_f following the ASTM D790 protocol [26]), flexural stiffness (D) and planar density (ρ). The facing stress and core shear stress are calculated following Eqs. (1) - (2) (ASTM C393 [27]):

$$F_s^{ult} = \frac{P_{max}}{(d+c)*b} \, [\text{MPa}] \qquad [1]$$

$$\sigma = \frac{P_{max}*S}{2*t*(d+c)*b} \, [\text{MPa}] \qquad [2]$$

Where P_{max} is the maximum force, d is the sandwich thickness, t is the nominal facing thickness, b is the sandwich width, S is the support span length and c is the core thickness (calculated from c = d – 2*t). The flexural strength σ_f and the flexural stiffness are obtained from Eqs. (3) - (4):

$$\sigma_f = \frac{3*P_{max}*S}{2*b*d^2} \, [\text{MPa}] \qquad [3]$$

$$D = \frac{PS^3}{48bw} \, [GPa] \tag{4}$$

Where w is the deflection of bending. Finally, the planar density of the sandwich panels can be determined on the basis of Eq. (5):

$$\rho = \frac{m}{A} \left[\frac{Kg}{m^2}\right] \tag{5}$$

where, m is the mass of the sandwich panel and A is the area of the nominal structure.

3. RESULTS

3.1 Hybrid composite – core material

Analysis of variance (ANOVA) is used to identify the effect of main and interactions of factors on the elastic flexural properties based on an 95% confidence interval. The main factor is only interpreted individually when there are no significant interaction effects. P-values less than or equal to 0.05 (α-level of 0.05) indicate the main factor or the interaction significantly affects the response. P-values underlined in Table reveal the significant factors affecting the response, while those highlighted in bold correspond to the higher-order interactions in which they will be illustrated via effect plots.

Table 4. Analysis of variance (ANOVA) for the particulate composite.

Experimental factor	Modulus of elasticity [GPa]	Flexural strength [MPa]
	P-values $\leq$ 0.05	
Fraction $\frac{\text{wood sawdust}}{\text{epoxy resin}}$ (wt%)	0.000	0.175
Cement Particles (wt%)	0.000	0.030
Fraction $\frac{\text{wood sawdust}}{\text{epoxy resin}}$ * Cement Particles	**0.010**	**0.011**

The modulus of elasticity of the wood sawdust-cement composite ranges from 1.91 GPa to 2.79 GPa. A second order interaction effect is significant, showing a P-value of 0.010 (see Table 4). Figure 11 shows the interaction effect plot for the mean elastic modulus response. Composites constituted of a smaller amount of epoxy resin (40/60) achieve superior stiffness, especially when a larger amount of cement particles is incorporated. This behaviour can be attributed to the lower epoxy polymer stiffness compared to wood and cement particles. In addition, a greater amount of matrix phase can hinder the rheology and packing of the system, affecting the effective mechanical

properties of the composite material. Cement particles can act as a filler, reducing the porosity of the system. Some authors [30-31] have reported a possible hydration of the cement grains when mixed with epoxy polymer. This effect can enhance the mechanical properties of the epoxy matrix phase, thus increasing the mechanical strength and stiffness of the composites. A higher modulus of elasticity is achieved when a particle/matrix fraction of 40/60 and 10 wt% of cement particles is considered.
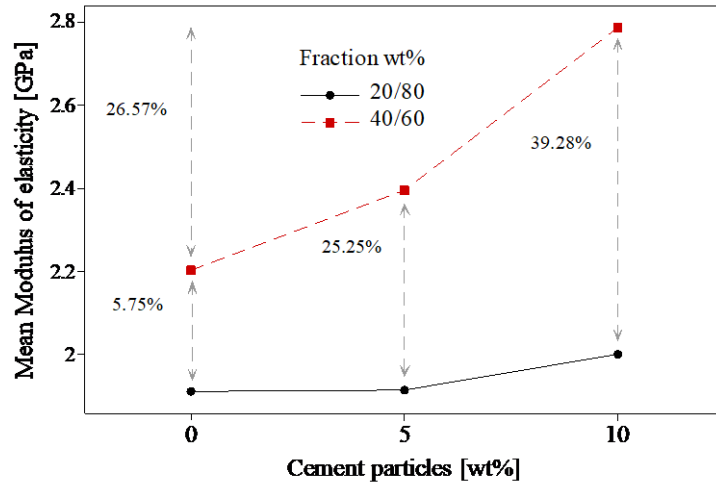

Figure 11. Interaction effect plot for mean elastic modulus.

The flexural strength of the hybrid composites ranges from 37.92 MPa to 46.97 MPa. An interaction of second order significantly affects the flexural strength, revealing a P-value (0.011) lower than 0.05 (Table 4). Figure 12 shows the interaction effect plot for the mean flexural strength. In general, the lower ratio of matrix phase (40/60) leads to an increase in flexural strength results. This effect is intensified when the hybrid composites are made with 10 wt% of cement particles, indicating a relevant percent increase of nearly 23.87%, which agrees with the stiffness results shown in Figure 9. This behaviour shows that the matrix phase at the lower level (60%) is still able to strengthen the composites when combined with the cement particles. Based on these results, the honeycomb core is composed and manufactured with a wood sawdust/epoxy resin level at 40/60 and cement particle inclusions at 10 wt%.
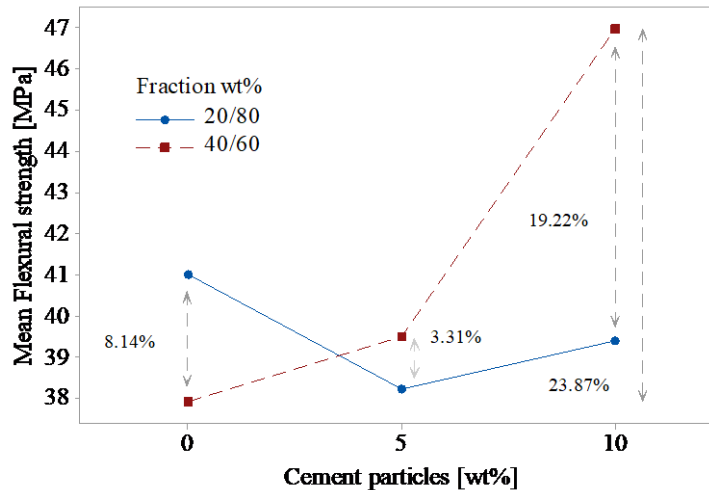
Figure 12. Interaction effect plot for mean flexural strength.

3.2 Parametric analysis for the sandwich panel

The numerical flexural strength data of the sandwich panel ranges from 18.67 MPa to 96.32 MPa. Figure 13 shows the behaviour of the flexural strength as a function of the geometric parameters of the honeycomb core. The increase in web and facing thickness provides higher strength (Fig. 13b, c), except when the height of the cell varies from 20 to 30 mm (Fig. 13d). A similar characteristic has been also verified by Wang *et al.* [32]. The increase in honeycomb-core thickness leads to increased surface area between core and facings, enhancing, consequently, the flexural performance of the panel. In addition, the increase number of honeycomb cells also affects the distribution of the contact area between the hybrid core and Piassava facings, which may improve the interfacial bonding condition. Oliveira *et al.* [33] has attributed the lower mechanical performance of the sandwich bottle cap panels to the reduced contact area between the metal sheets and the cylindrical honeycomb cores.

Error! Reference source not found.a, 13b, 13c and 13d reveal that the honeycomb configuration (rectangular and hexagonal) has little effect on the flexural strength of the panels. The rectangular configuration reached a strength slightly higher than the hexagonal geometry. In this way, the decrease of the surface area obtained by the rectangular geometry contributes to increase the flexural strength of the panels.

Error! Reference source not found.3e, 13f and 13g show that the increase in flexural strength is primarily associated with the increase in the cross-sectional area (number of cells) of the honeycomb core, reducing the void volume of the cells. The lower number of cells (42) leads to the reduction of flexural strength compared to the

larger number of cells, demonstrating that cell density plays an important role in the bending behaviour of the panel.
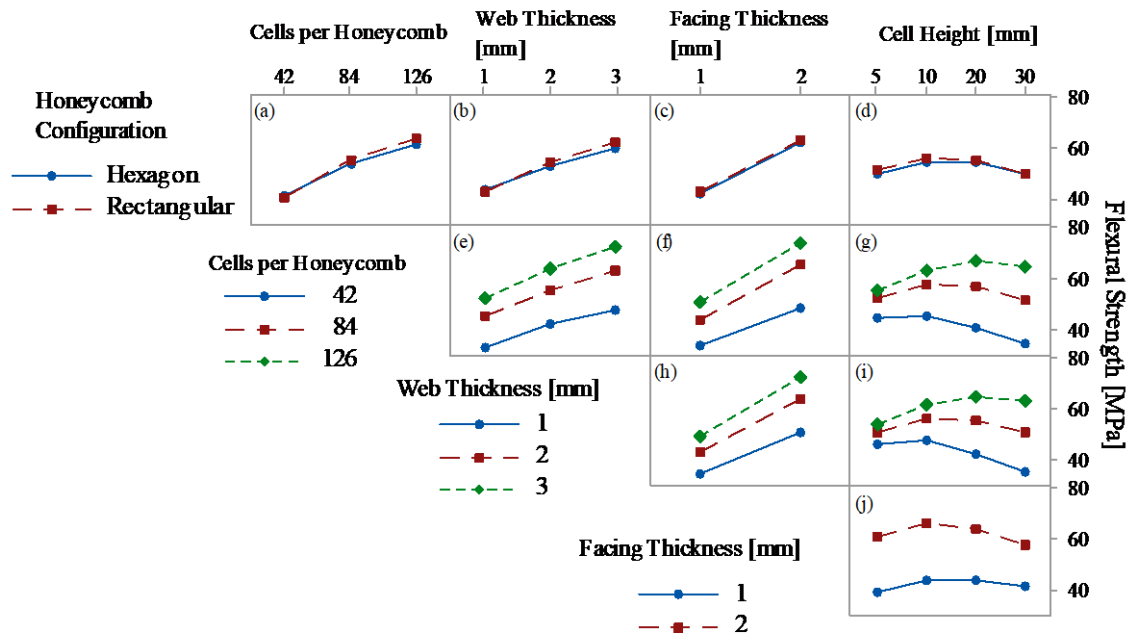

Figure 13. Interactions of the geometric factors on the flexural strength of the panels.

Figure 14 shows the relationships between the honeycomb geometric parameters and the flexural stiffness of the sandwich panels. In general, the numerical stiffness is increased when the honeycomb thickness and density (number of honeycomb-cells) increase. The honeycomb configuration does not affect the panel stiffness, achieving similar behaviours, such as those shown in Figures 14a, b, c and d. This behaviour implies that both honeycomb configurations are largely dependent on the mass distribution. According to Yu *et al.* [34] when the mass distribution is concentrated towards symmetry in-plane, the stiffness and strength of the sandwich are significantly improved. An increment in flexural stiffness is revealed by the increase in web thickness and cell size factors (see Figure 13e, f, g). Gholami *et al.* [35] investigated the effects of the aspect ratio, load and allowable deflection of the plate on the honeycomb optimal design, revealing that the optimal configuration is based on a minimum cross section (high number of cells) and maximum allowable length. The effect of the area moment of inertia is also noted in Figure 13g, i, j, showing a large variation in flexural stiffness when the cell height is increased. However, this variation is not uniform between the cell height levels, which implies the presence of interaction effects of the factors.
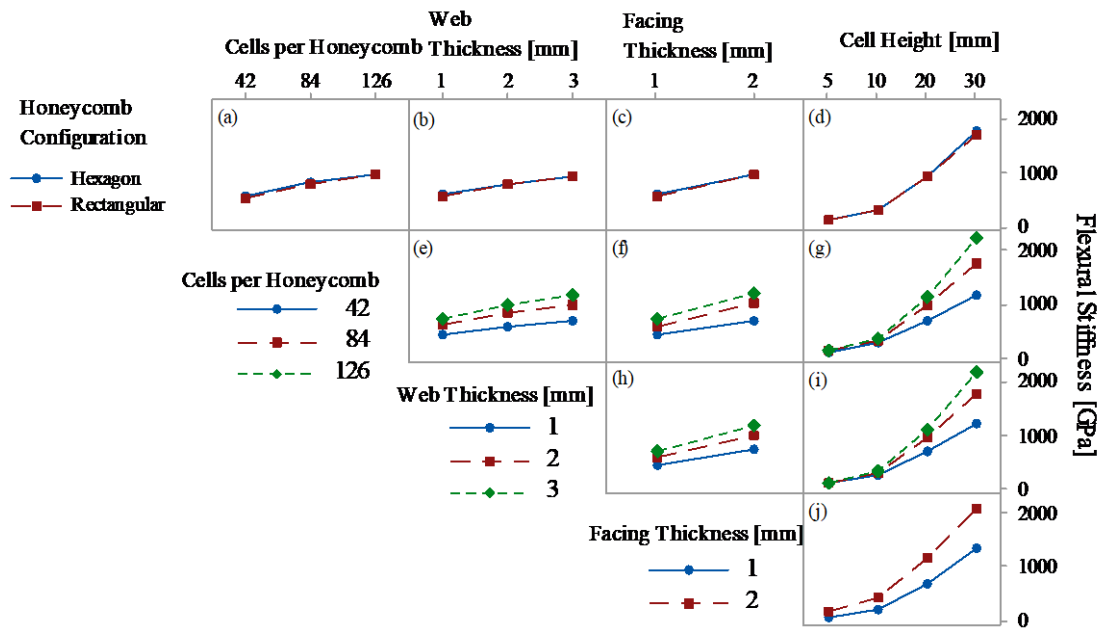
Figure 14. Interactions between the geometric factors on the panel flexural stiffness.

It is well known that the sandwich panel strength depends on the facing and core elastic properties, the facing-core interface bonding and inertia effects [36-37]. Figures 14 and 15 show the relationship of the parametric entities for the facing and core shear stresses of the sandwich panels, respectively. The facing and core shear stresses presented similar behaviours in relation to the flexural strength and stiffness. The facing and core shear stresses are predominately associated with the variation of the web thickness (h-i), cell height (g,i,j) and cross-sectional area (e,f,g,j), instead of the honeycomb geometries(a-d). The results shown in Figures 15, 16a-d demonstrate that the facing and core shear stresses are independent of the honeycomb configuration. The thickness of the laminate layer reveals different effects on the facing stress (Fig. 15j) and core shear stress (Fig. 16j). The thicker laminate provides lower skin stress, which can be attributed to the facing thickness and stress parameters being inversely proportional, as presented in Equation 2.
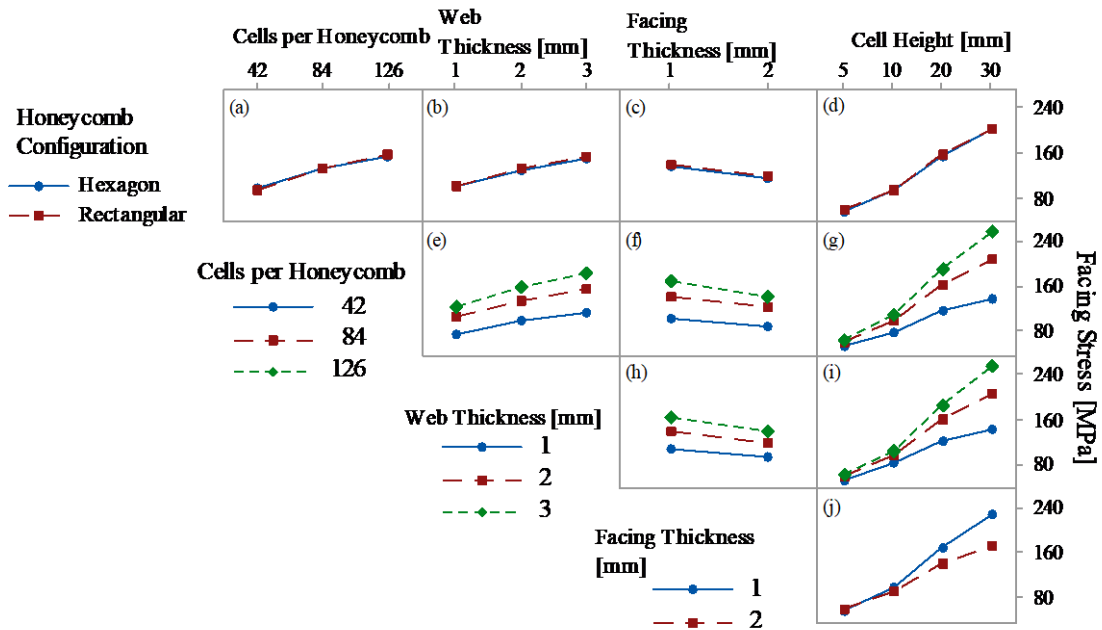
Figure 15. Relation of the geometric factors with the facing stress.
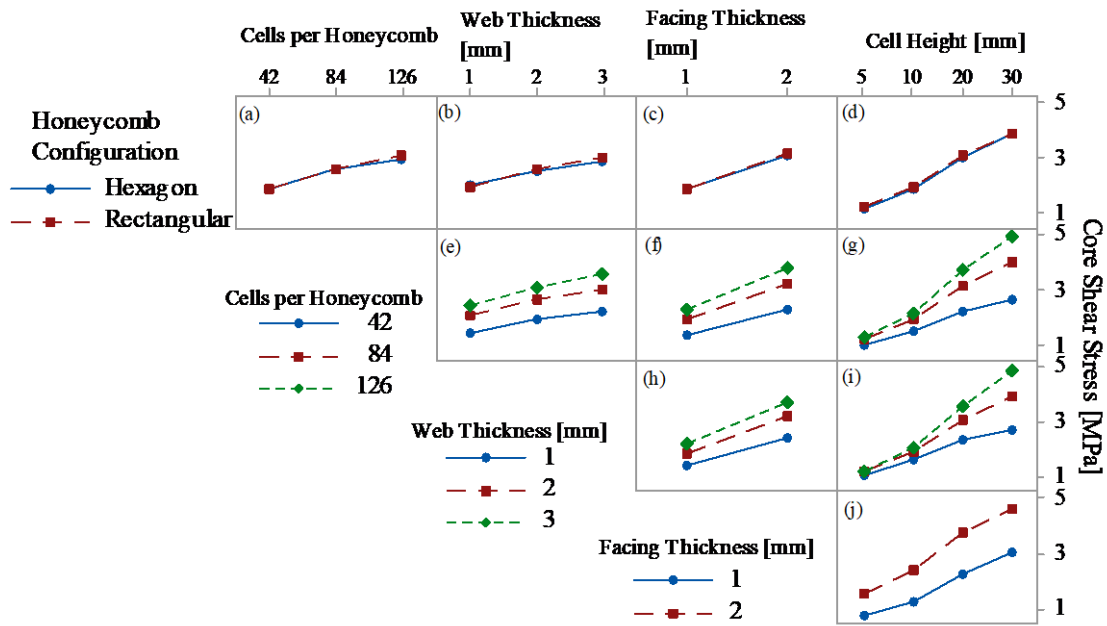
Figure 16. Relation of the geometric factors with the core shear stress.

Figure 17 shows the relation of the parametric entities for the density of the sandwich panels. The planar density of the sandwich panel varied from 2.33 kg/m² to 18.81 kg/m². In general, the increase of the geometric cell parameters leads to higher densities. The rectangular honeycomb density is slightly higher than hexagonal configuration (Figure 17 a, b, c, d). A denser structure is achieved when the higher levels of facing thickness, web thickness and cell height factors are considered. It is possible to identify a relationship between density (Figure 17) and flexural stiffness

(Figure 14) responses. The non-uniform density variations between cell height levels against cell density (Figure 17g) and web thickness (Figure 17i) levels also demonstrate the presence of interaction effects. Higher facing thickness provides higher density showing a linear and similar behaviour against cell height factor (Figure 17j). In contrast, this factor does not affect linearly the flexural stiffness and strength responses as shown in Figures 14j and 15j.
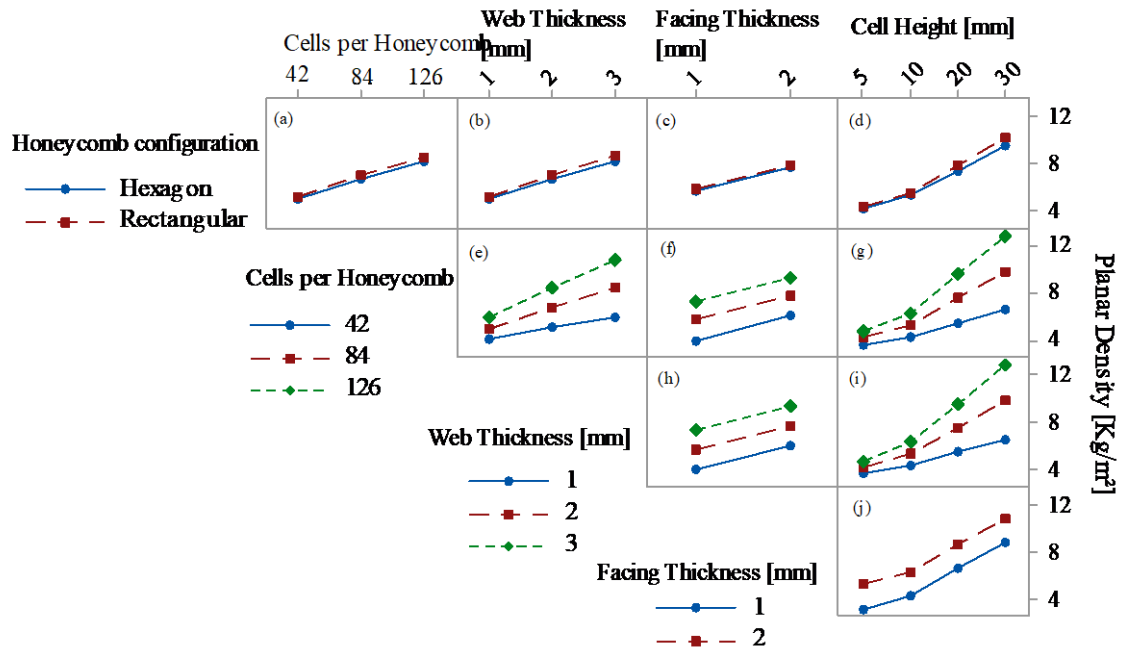

Figure 17. Relation of the geometric factors with the panel planar density.

3.3 Comparative and fracture analysis

This section shows a comparative analysis between the proposed panels and three polymer core sandwich structures, (i) sisal polypropylene (PP) core with 3 and 6-ply wood veneer facings [36], (ii) all-PP honeycomb panel [37] and (iii) PP-honeycomb core with aluminium skins [33], under three-point bending. The piassava sandwich panels achieve superior properties when compared to the sisal-PP [36], all-PP [37] and aluminium-PP [33] sandwich panels, as shown in Table 6. This comparison indicates that piassava composite facings are promising, since the sandwich panels reach greater strength and stiffness with respect to the PP-aluminium structure [33]. In addition, the sawdust composite core achieves acceptable mechanical performance compared to the PP cores.

Table 6. Comparative analysis between the proposed panels and similar works.

| Responses | Hexagon | Rectangular | Rao et al. [35] | | Cabrera et al. [36] | Oliveira et al. [32] |
			Sisal-PP core (6-ply)	Sisal-PP core (3-ply)	PP-honeycomb	PP-Aluminium
Flexural Strength (MPa)	73.3	62			20.66	24.3 (2.4)
Flexural Stiffness (MPa)	4267.07	4907.8	271.86	176.92	56.92	2490 (15)
Core shear stress (MPa)	**1.41(0.11)**	**1.22(0.13)**	**1.45(0.1)**	**1.31(0.17)**	**0.14**	0.77 (0.06)
Facing stress (MPa)	71.97(2.16)	62.31(3.47)	30.42(2.16)	31.93(4.16)	30	115 (9.7)

A buckling effect of the PP-honeycomb panels under bending was reported by Cabrera [37]. The piassava sandwich panels do not present buckling. The failure of the proposed panels is initiated by a localised rupture of the hybrid core as shown in Figure 18. The crack propagates from the centre of the core to the interface with a subsequent drop in bending force. In general, hexagonal core panels do not exhibit delamination of the skins. In some cases, a delamination of the upper composite skin occurs when the rectangular core is used. This behaviour implies that the rectangular cell configuration is less effective on the bonding interface. Although the hexagonal and rectangular cells have similar contact area with the skins, the hexagon cell has a diagonal cell wall that may be responsible for a more uniform stress distribution at the interface. It is worth noting that no delamination occurs in the lower skins. Oliveira et al. [33] also reported delamination of the upper aluminium skin.

(a)

(b)

Figure 18. Failure analysis for rectangular (a) and hexagon panels (b).

4. CONCLUSIONS

The main conclusions are following described:

i.   The interaction of the factors "sawdust mass fraction and cement particles" significantly affects the flexural strength and stiffness of the hybrid composites. The composite consisted of less epoxy resin (40/60) and higher cement particle content (10 wt%) achieved higher stiffness values.

ii. The rectangular and hexagonal honeycomb core configurations provide similar flexural stiffness values. However, the rectangular honeycomb reveals a slight increase in flexural strength, facing stress and core shear stress.

iii. The hybrid core is the first to fail by shear, with a subsequent drop in bending force. No delamination occurs for hexagonal core panels, while some are observed for the rectangular core panels.

iv. The planar density, flexural strength and stiffness of the sandwich panels have a strong dependence on the geometric variations of the cells. The higher levels of parametric institutions lead to an increase in bending stiffness and density. Higher flexural strength of the sandwich panels is obtained when the height of the cell ranges from 20 to 30 mm. Parametric analysis reveals that the stiffness of the sandwich panel mainly depends on the facing thickness, web thickness, cell height and honeycomb density. The non-uniform and non-linear behaviours between them imply the presence of interaction effect on the stiffness response.

v. The facing and core shear stresses of the panels achieve a similar tendency for flexural strength and stiffness. The web thickness, cell size and cross section area characteristics have a strong relationship with the elastic properties of the sandwich beam. The thicker core and the larger number of cells contribute to better inertia performance.

vi. Sustainable sandwich panels achieved promising properties for secondary structural applications. This material allows the recycling of a relevant amount of wood wastes, besides the use of Piassava fibres, which contributes to the innovative development of new pro-ecological technologies.

ACKNOWLEDGEMENTS

REFERENCES

[1] Russell, B.P.; Liu, T.; Fleck, N.A. and Deshpande, V.S. 'Quasi-static three-point bending of carbon fiber sandwich beams with square honeycomb cores'. *Journal of Applied Mechanics* **78**, (2011) 0310081-03100815. doi: 10.1115/1.4003221

[2] Hou, Y.; Tai, Y.H.; Lira, C.; Scarpa, F.; Yates, J.R. and Gu, B. 'The bending and failure of sandwich structures with auxetic gradient cellular cores'. *Composites Part A: Applied Science and Manufacturing* **49** (2013) 119-131. doi: https://doi.org/10.1016/j.compositesa.2013.02.007

[3] Davalos, J.F.; Qiao, P.; Frank, X.X.; Robinson, J. and Barth, K.E. 'Modeling and characterization of fibre-reinforced plastic honeycomb sandwich panels for highway bridge applications'. *Composite Structures* **52** (2001) 441-52. doi: https://doi.org/10.1016/S0263-8223(01)00034-4

[4] Menta, V.V.K.; Vuppalapati, R.R.; Chandrashekhara, K.; Pfitzinger, D. and Phan, N. 'Manufacturing and mechanical performance evaluation of resin-infused honeycomb composites'. *Journal of Reinforced Plastics and Composites* **31** (2012) 415-23. doi: https://doi.org/10.1177/0731684412439792

[5] Coburn, B.H. and Weaver, P.M. 'Buckling analysis, design and optimisation of variable-stiffness sandwich panels'. *International Journal of Solids and Structures* **96** (2016) 217-228. doi: https://doi.org/10.1016/j.ijsolstr.2016.06.007

[6] Du, Y.; Yan, N. and Kortschot, M.T. 'An experimental study of creep behavior of lightweight natural fibre-reinforced polymer composite/honeycomb core sandwich panels'. *Composite Structures* **106** (2013)160-6. doi: https://doi.org/10.1016/j.compstruct.2013.06.007

[7] Sun, G., Huo, X., Chen, D., Li, Q. 'Experimental and numerical study on honeycomb sandwich panels under bending and in-panel compression'. *Materials & Design*, 133 (2017) 154-168. doi: https://doi.org/10.1016/j.matdes.2017.07.057

[8] Wang, Z., Li, Z., Xiong, W. 'Numerical study on three-point bending behavior of honeycomb sandwich with ceramic tile'. *Composites Part B: Engineering*, 167 (2019) 63-70. doi: https://doi.org/10.1016/j.compositesb.2018.11.108

[9] Reis, J.M.L. and Carneiro, E.P. 'Effect of Piassava lees in the fracture behavior of polymer mortars'. *Composite Structures*, **95** (2013) 564-568. doi: https://doi.org/10.1016/j.compstruct.2012.07.008

[10] Dai. D. and Fan. M. 'Preparation of bio-composite from wood sawdust and gypsum'. *Industrial Crops and Products,* **74** (2015) 417-424. doi: https://doi.org/10.1016/j.indcrop.2015.05.036

[11] Nascimento, D.C.O., Ferreira, A.S., Monteiro, S.N., Aquino, R.C.M.P. and Kestur, S.G. 'Studies on the characterization of piassava fibers and their epoxy composites'. *Composites Part A: Applied Science and Manufacturing* **43** (2012) 353-362. doi: https://doi.org/10.1016/j.compositesa.2011.12.004

[12] Ravi, M. R.; Jhalani, A.; Sinha, S. and Ray, A. 'Development of a semi-empirical model for pyrolysis of an anular sawdust bed'. *Journal of Analytical Applied Pyrolysis* **74** (2004) 353-374. doi: https://doi.org/10.1016/S0165-2370(03)00102-5

[13] Herai, Y.; Kouno, K.; Hashimoto, M. and Nagaoka, T. 'Relationships between microbial biomass nitrogen, nitrate leaching and nitrogen uptake by corn in a compost and chemical fertilizer-amended regosol'. *Soil Science Plant Nutrition,* **52** (2006) 186-194. doi: https://doi.org/10.1111/j.1747-0765.2006.00031.x

[14] Felix, J.S.; Demoño, C. and Nerín, C. 'Characterization of wood plastic composites made from landfill-derived plastic and sawdust: volatile compounds and olfactometric analysis'. *Waste Manage* **33** (2013) 645-6. doi: https://doi.org/10.1016/j.wasman.2012.11.005

[15] Hisham, S.; Faieza, A.A.; Ismail, N.; Sapuan, S.M. and Ibrahim, M.S. 'Flexural mechanical characteristic of sawdust and chipwood filled epoxy composites'. *Composite Science Technology*, **471-472** (2011) 1064-1069. doi: https://doi.org/10.4028/www.scientific.net/KEM.471-472.1064

[16] Pérez, E.; Famá, L.; Pardo, S.G.; Abad, M.J. and Bernal, C. 'Tensile and fracture behaviour of PP/wood flour composites'. *Composites Part B: Engineering* **43**, (2012) 2795-800. doi: https://doi.org/10.1016/j.compositesb.2012.04.041

[17] Ku, H.; Prajapati, M. and Cardona, F. 'Thermal properties of sawdust reinforced vinyl ester composites post-cured in microwaves: a pilot study'. *Composites Part B: Engineering*, **42** (2011)898-906. doi: https://doi.org/10.1016/j.compositesb.2011.01.008

[18] Missagia, Z. M. V., Santos, J. C., Panzera, T. H., Brandão, L. C., Silva, D. A. L. and Christoforo, A. 'Particulate composite material in epoxy matrix reinforced with sawdust, cement and magnesium silicate'. *Ambiente Construído,* **13** (2013)285-302. doi: http://dx.doi.org/10.1590/S1678-86212013000300017

[19] Melo, A.B.L., Panzera, T.H., Freire, R.T.S. and Scarpa, F. 'The effect of Portland cement inclusions in hybrid glass fibre reinforced composites based on a full factorial design'. *Composite Structures* **202** (2018) 233-240. doi: https://doi.org/10.1016/j.compstruct.2018.01.069

[20] Torres, R.B., Santos, J.C. Panzera, T.H., Christoforo, A.L., P.H.R. Borges, F. Scarpa, 'Hybrid glass fibre reinforced composites containing silica and cement microparticles based on a design of experiment'. *Polymer Testing* **57** (2017) 87-93. doi: https://doi.org/10.1016/j.polymertesting.2016.11.012

[21] Ribeiro Filho, S.L.M., Oliveira, P.R., Vieira, L.M.G., Panzera, T.H., Freire, R.T.S. and Scarpa, F. 'Hybrid bio-composites reinforced with sisal-glass fibres and Portland cement particles: A statistical approach'. *Composites Part B: Engineering* **149** (2018) 58-65. doi: https://doi.org/10.1016/j.compositesb.2018.05.019

[22] Elzubair, A. and Suarez, J.C.M. 'Mechanical behavior of recycled polyethylene/Piassava fibre composites'. *Materials Science and Engieering: A* **557** (2012) 29-35. doi: https://doi.org/10.1016/j.msea.2012.06.051

[23] D'Almeida, A.L.F.S.; D'Almeida, J.R.M.; Barreto, D.W. and Calado, V. J. 'Effect of surface treatments on the thermal behavior and tensile strength of Piassava (*Attalea funifera*) fibres'. *Applied Polymer Science* **120** (2011) 2508-2515. doi: https://doi.org/10.1002/app.33349

[24] Monteiro, S.N. 'Properties and structure of Attalea funifera (Piassava) fibres for composite reinforcement – a critical discussion'. *Nat Fibres* **6** (2008)191-203. doi: https://doi.org/10.1080/15440470902961128

[25] Elzubair, A.; Bonelli, C.M.C.; Rademaker, H.; Suarez, J.C.M. and Mano, E.B. 'Morphological, structural, thermal and mechanical characterization of Piassava

fibres'. *Journal of Natural Fibres*, **4** (2007) 13-31. doi: https://doi.org/10.1300/J395v04n02_02

[26] ASTM, AMERICAN SOCIETY FOR TESTING AND MATERIALS. ASTM D790: Standard Test Methods for Flexural Properties of Unreinforced and Reinforced Plastics and Electrical Insulating Materials, 2015. doi: 10.1520/D0790-17

[27] ASTM, AMERICAN SOCIETY FOR TESTING AND MATERIALS. C393/C393M–11: Standard Test Method for Core Shear Properties of Sandwich Constructions by Beam Flexure, 2011. doi: 10.1520/C0393_C0393M-16

[28] Dadej, K. and Surowska, B. 'Analysis of cohesive zone model parameters on response of glass epoxy composite in mode II interlaminar fracture toughness test'. *Composites theory and practice*, 16 (2016) 180-188.

[29] Turgut, P. 'Cement composites with limestone dust and different grades of wood sawdust'. *Building and Environment*, 42 (2007) 3801-3807. doi: https://doi.org/10.1016/j.buildenv.2006.11.008

[30] Panzera, T.H., Sabariz, A.L.R., Strecker, K., Borges, P.H.R., Vasconcelos, D.C.L. and Wasconcelos, W. L. 'Mechanical properties of composite materials based on Portland cement and epoxy resin'. *Cerâmica* **56** (2010) 77-82. doi: http://dx.doi.org/10.1590/S0366-69132010000100013

[31] Martuscelli C.C., Santos, J.C., Oliveira, P.R., Panzera, T.H. Aguilar, M.T.P. and Garcia, C.T. 'Polymer-cementitious composites containing recycled rubber particles'. *Construction and Building Materials* **170** (2018) 446-454. doi: https://doi.org/10.1016/j.conbuildmat.2018.03.017

[32] Wang, J., Shi, C., Yang, N., Sun, H., Liu, Y. and Song, B. 'Strength, Stiffness, and Panel Peeling Strength of Carbon Fiber-Reinforced Composite Sandwich Structures with Aluminum Honeycomb Cores for vehicle body'. *Composite Structures* (2017), doi: https://doi.org/10.1016/j.compstruct.2017.10.038.

[33] Oliveira, P.R., Panzera, T.H., Freire, R.T., and Scarpa, F. 'Sustainable sandwich structures made from bottle caps core and aluminium skins: A statistical

approach'. *Thin-Walled Structures,   130*   (2018)   362-371.   doi: https://doi.org/10.1016/j.tws.2018.06.003

[34] Yu, B., Han, B.; Su, P.B.; Ni, C.Y.; Zhang, Q.C. and Lu, T.J. 'Graded square honeycomb as sandwich core for enhanced mechanical performance'. *Materials & Design* **89** (2016) 642-652. doi: https://doi.org/10.1016/j.matdes.2015.09.154

[35] Gholami, M.; Alashti, R.A. and Fathi, A. 'Optimal design of a honeycomb core composite sandwich panel using evolutionary optimization algorithms'. *Composite   Structures*   **139**   (2016)   254-262.   doi: https://doi.org/10.1016/j.compstruct.2015.12.019

[36] Rao, S., K. Jayaraman, K., and Bhattacharyya, D. 'Micro and macro analysis of sisal fibre composites hollow core sandwich panels'. *Composites Part B: Engineering*,   43   (2012)   2738-2745.   doi: https://doi.org/10.1016/j.compositesb.2012.04.033

[37] Cabrera, N.O., Alcock, B., Peijs, T. 'Design and manufacture of all-PP sandwich panels based on co-extruded polypropylene tapes'. *Composites Part B: Engineering*.   39   (2008)   1183–1195.   doi: https://doi.org/10.1016/j.compositesb.2008.03.010